

Machine learning the dynamics of quantum kicked rotor

Tomohiro Mano, Tomi Ohtsuki

Physics Division, Sophia University, Kioicho 7-1, Chiyoda-ku, Tokyo 102-8554, Japan

Abstract

Using the multilayer convolutional neural network (CNN), we can detect the quantum phases in random electron systems, and phase diagrams of two and higher dimensional Anderson transitions and quantum percolations as well as disordered topological systems have been obtained. Here, instead of using CNN to analyze the wave functions, we analyze the dynamics of wave packets via long short-term memory network (LSTM). We adopt the quasi-periodic quantum kicked rotors, which simulate the three and four dimensional Anderson transitions. By supervised training, we let LSTM extract the features of the time series of wave packet displacements in localized and delocalized phases. We then simulate the wave packets in unknown phases and let LSTM classify the time series to localized and delocalized phases. We compare the phase diagrams obtained by LSTM and those obtained by CNN.

Keywords: Anderson transition, quantum phase transition, quantum kicked rotor, machine learning, convolutional neural network, long short-term memory network

1. Introduction

Critical behaviors of the Anderson transition[1] have been attracting considerable attention for more than half a century. The problem is related to quantum percolation[2, 3, 4, 5, 6], where the wave functions on the randomly connected lattice sites begin to be extended [7]. Electron states on random lattice systems are difficult to study, because the conventional methods of using the transfer matrix[8] are not applicable. The scaling analyses of the energy level statistics[9] are also difficult, if not impossible[10, 11], owing to the spiky density of states [6].

¹⁰ To overcome these difficulties, neural networks[12, 13, 14, 15] to classify the states [16, 17, 18, 19, 20, 21, 22, 23, 24, 25, 26] had been used. That is, instead of classifying images of photos, we input the wave functions (actually the squared modulus of them) at the Fermi energy and classify them to metal, insulator, topological insulator etc. First we train the convolutional neural network in

Email address: ohtsuki@sophia.ac.jp (Tomi Ohtsuki)

Anderson model of localization, whose phase diagram is well known. We then apply the CNN to classify the eigenfunctions of quantum percolation to metal or insulator relying on the generalization capability of CNN. We have shown in refs. [27, 28] that this method is free from the above difficulties and works well in determining the phase diagrams of quantum percolation.

20 The above method, however, requires many eigenfunctions, which are difficult to obtain in higher dimensions. One of the way to study the Anderson transition without diagonalizing the Hamiltonian is to use quantum kicked rotor (QKR) [29, 30, 31], where we analyze the wave packet dynamics in one dimension. The simple quantum kicked rotor can be mapped to one-dimensional (1D) Anderson model[32], whereas with incommensurate modulation of the strength of kick, the model is mapped to tight binding models in higher dimensions[33].

In this paper, we draw phase diagrams of the three dimensional (3D) and four dimensional (4D) tight binding models that correspond to the QKR using the CNN trained for standard Anderson models of localization. We also analyze 30 the time series of QKR via long short-term memory (LSTM) network[34, 35], let LSTM classify the time series to localized/delocalized phases, draw the phase diagrams, and compare them with those drawn by the CNN analyses of tight binding models. We demonstrate that the phase boundaries of localized and delocalized phases are less noisy in the case of LSTM.

2. Model and Method

We consider QKR with incommensurate modulation of the kick as follows;

$$H(t) = \frac{p^2}{2} + K \cos x \times \sum_n \delta(t - n) \times F(t), \quad (1)$$

with

$$F(t) = \begin{cases} 1 + \epsilon \cos(\omega_2 t + \theta_2) \times \cos(\omega_3 t + \theta_3) & \text{3D} \\ 1 + \epsilon \cos(\omega_2 t + \theta_2) \times \cos(\omega_3 t + \theta_3) \times \cos(\omega_4 t + \theta_4) & \text{4D} \end{cases} \quad (2)$$

where ω_i are irrational numbers that are incommensurate with each other, K the strength of the kick, ϵ the modulation strength, and θ_i the initial phases.

40 We took $\omega_2 = 2\pi\sqrt{5}$, $\omega_3 = 2\pi\sqrt{13}$ and $\omega_4 = 2\pi\sqrt{23}$ [29, 30, 31].

We analyze the QKR in two ways. One way is to map this model to tight binding models,

$$H_{\text{tb}} = \sum_m \varepsilon_m |m\rangle \langle m| + \sum_{m,r} W_r |m\rangle \langle m-r|, \quad (3)$$

with $m = (m_1, m_2, m_3)$, $\varepsilon_m = \tan \left[-\frac{1}{2} (m_1^2 \hbar / 2 + \omega_2 m_2 + \omega_3 m_3) \right]$ and W_{r_1, r_2, r_3} the Fourier transform of $W(x_1, x_2, x_3) = \tan \left[\frac{K \cos x_1 (1 + \epsilon \cos x_2 \cos x_3)}{2\hbar} \right]$ for 3D [30, 32]. For 4D, we include m_4, r_4 and x_4 in a straightforward way. We diagonalize H_{tb} numerically to obtain the eigenfunctions, and let CNN determine whether

they are localized or delocalized. Details of the CNN method is reviewed in ref. [14]. Note that H_{tb} is defined on 3D cubic lattice for the case of two incommensurate frequencies (ω_2 and ω_3), whereas it is on 4D hypercubic lattice in the case of three incommensurate frequencies (ω_2, ω_3 , and ω_4). Note also that we use CNN that has been trained for Anderson models of localization [27, 14].

The other way is to solve the time dependent Schrödinger equation

$$i\hbar \frac{d}{dt} \psi(t) = H(t) \psi(t), \quad (4)$$

with \hbar set to 2.89[29, 30, 31], calculate the time dependence of “displacement” in momentum space,

$$p^2(t) = \langle \psi(t) | p^2 | \psi(t) \rangle, \quad (5)$$

and analyze the time series of $p^2(t)$ via LSTM. To follow the wave packet time evolution from $t = n + \eta$ to $t = n + 1 + \eta$ with η infinitely small positive number, we use

$$\psi(n+1) = \exp\left(-i \frac{K F(n+1) \cos x}{\hbar}\right) \times \exp\left(-i \frac{p^2}{2\hbar}\right) \psi(n). \quad (6)$$

We work in the p -space, and the multiplication of $\exp(-ia \cos x)$ ($a = KF(n+1)/\hbar$) is expanded in the p -space as $\langle p | \exp(-ia \cos x) | p' \rangle$, which is expressed by Bessel functions.

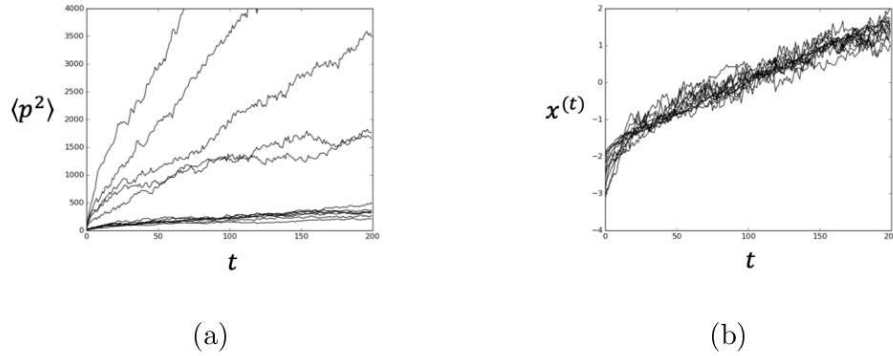


Figure 1: $p^2(t)$ vs. t for various K and ϵ with two incommensurate frequencies (3D case). (a) the plot before normalization. $p^2(t)$ is proportional to t for delocalized states, whereas it saturates to finite values for localized states. (b) after normalizing $p^2(t)$ to $x(t)$, the mean and standard deviation of which are 0 and 1, respectively. We have calculated the wave packet dynamics up to $T = 10^4$ time steps, and recorded $p^2(t)$ at every 50 time steps.

3. Results

We first apply the CNN trained for the Anderson model to the wave functions obtained by diagonalizing Eq. (3). For 3D systems, the system size is $32 \times 32 \times$

32, whereas for 4D it is $10 \times 10 \times 10 \times 10$. We diagonalize the systems with periodic boundary conditions, obtain the eigenfunctions at the center of the energy spectrum, input squared modulus of the eigenfunctions to the CNN, and let CNN calculate the probabilities for the inputs being delocalized. The results are shown in Fig. 2 (a) (3D) and (c) (4D) as a heat map.

We next analyze the time series of $p^2(t)$, Fig. 1. We first note that

$$p^2(t) \sim \begin{cases} Dt & \text{delocalized,} \\ \xi^2 & \text{localized,} \\ t^{2/d} & \text{critical,} \end{cases} \quad (7)$$

70 with D the diffusion constant, ξ the localization length, and d the dimension. At the critical point, $p^2(t) \propto t^{2/d}$, so for 3D $p^2(t) \propto t^{2/3}$ and for 4D $p^2(t) \propto t^{1/2}$ [36]. Note that we discuss here the localization/delocalization in momentum space.

We find the critical strength (K, ϵ) by detecting the behaviors $p^2(t) \propto t^{2/d}$, and use this information for supervised training of LSTM. The values of $p^2(t)$, however, strongly depend on K and ϵ , and the neural network tends to learn only maxima and minima of $p^2(t)$. We therefore preprocessed the data by normalizing them, i.e., normalize $p^2(t)$ to $x^{(t)}$, whose mean and standard deviation are 0 and 1, respectively.

80 We first determine the critical point along a straight line in ϵ - K plane by finding a point that shows $p^2(t) \propto t^{2/d}$ (see white crosses in Fig. 2). Once the critical point is determined, we prepare time series $p^2(t)$ for localized and delocalized phases by varying (K, ϵ) along a straight line indicated by green arrows in Fig. 2(b),(d). We then normalize $p^2(t)$ to $x^{(t)}$ and use them for training bidirectional LSTM. Once the LSTM is trained, we vary parameters in ϵ - K plane and calculate $x^{(t)}$, and feed $x^{(t)}$ to LSTM, which outputs the probability that the input time series $x^{(t)}$ belongs to the delocalized phase. The results are shown in Fig. 2(b) for 3D and Fig. 2(d) for 4D, which nicely distinguish localized and delocalized phases.

90 Now we compare the phase diagrams (heat maps) for 3D and 4D systems. In the case of 3D, both CNN and LSTM give reasonably sharp phase boundaries [see Fig. 2(a), (b)]. On the other hand, in the case of 4D, the phase boundary becomes noisy if we use 4D CNN [Fig. 2(c)]. This is because in the case of 4D, only small system can be diagonalized, and CNN fail to learn the detailed features of localized and delocalized states. In the case of LSTM [Fig. 2(d)], the phase boundary is less noisy, since we do not need to diagonalize the system, and we can follow as long time series as in 3D case.

4. Summary

100 To summarize, we have analyzed the quantum kicked rotor with time modulated kick strength. The systems are analyzed in two ways. One is to map the Hamiltonian to static higher dimensional tight binding models and study the eigenfunctions via the deep convolutional neural network. The other is to analyze the time series of the original time dependent one dimensional systems

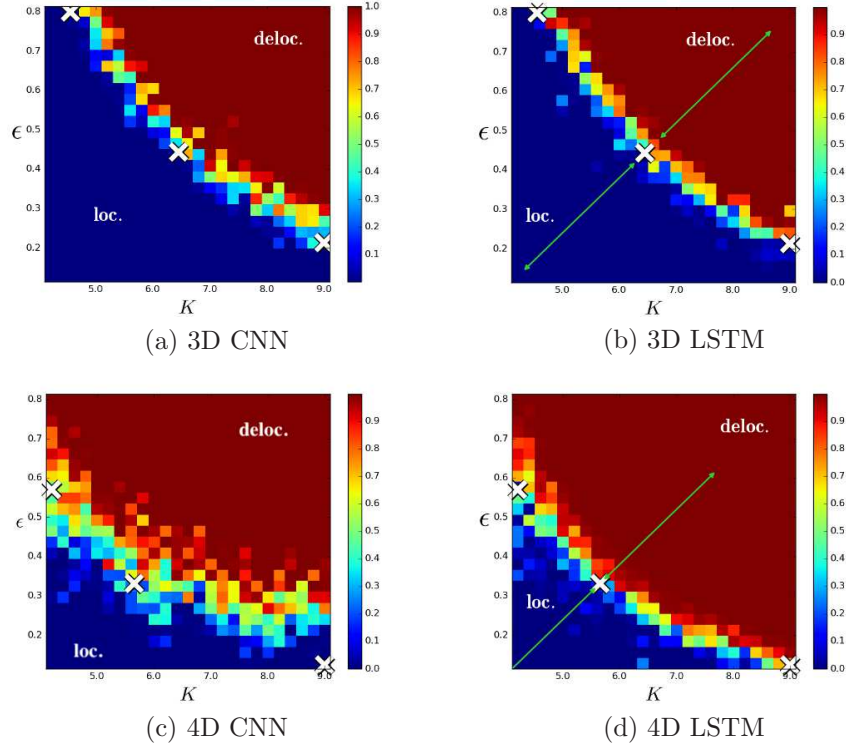


Figure 2: Phase diagrams of QKR in ϵ - K plane. At each (K, ϵ) , we plot the probability that the parameter belongs to the delocalized phase. Those obtained by CNN[(a) and (c)] and those by LSTM[(b) and (d)]. 3D cases [(a) and (b)] and 4D cases[(c) and (d)]. The CNN is trained by Anderson model of localization. The training regions of LSTM are indicated as green arrows. White crosses are obtained by the critical behaviors of $p^2(t)$. In all cases, average over 5 samples has been taken. Random choice of $0 \leq \theta_i < 2\pi$ and random shift of $(m_1, m_2, \dots) \rightarrow (m_1 + \beta_1, m_2 + \beta_2, \dots)$, $0 \leq \beta_i < 1$ have been performed[30].

via bidirectional long short-term memory network. We have demonstrated that the latter approach gives less noisy phase boundary between the localized and delocalized phases. The latter approach works especially well for analyzing the Anderson transitions in higher dimensions.

Acknowledgement This work was supported by JSPS KAKENHI Grant Nos. 16H06345, and 19H00658. We thank Dr. Matthias Stosiek for critical reading of the manuscript.

110 References

- [1] P. W. Anderson, Absence of diffusion in certain random lattices, Phys. Rev. 109 (1958) 1492.
- [2] S. Kirkpatrick, T. P. Eggarter, Localized states of a binary alloy, Phys. Rev. B 6 (1972) 3598–3609.
- [3] A. Sur, J. L. Lebowitz, J. Marro, M. H. Kalos, S. Kirkpatrick, Monte carlo studies of percolation phenomena for a simple cubic lattice, Journal of Statistical Physics 15 (1976) 345–353.
- [4] G. Schubert, A. Weiße, G. Wellein, H. Fehske, HQS@HPC: Comparative numerical study of Anderson localisation in disordered electron systems, Springer Berlin Heidelberg, Berlin, Heidelberg, 2005, pp. 237–249. URL: https://doi.org/10.1007/3-540-28555-5_21. doi:10.1007/3-540-28555-5_21.
- [5] A. Aharony, D. Stauffer, Introduction To Percolation Theory: Revised Second Edition, Taylor & Francis, London, 1994.
- [6] L. Ujfalusi, I. Varga, Finite-size scaling and multifractality at the anderson transition for the three wigner-dyson symmetry classes in three dimensions, Phys. Rev. B 91 (2015) 184206.
- [7] T. Makiuchi, M. Tagai, Y. Nago, D. Takahashi, K. Shirahama, Elastic anomaly of helium films at a quantum phase transition, Phys. Rev. B 98 (2018) 235104.
- [8] K. Slevin, T. Ohtsuki, Critical exponent for the anderson transition in the three-dimensional orthogonal universality class, New Journal of Physics 16 (2014) 015012.
- [9] B. I. Shklovskii, B. Shapiro, B. R. Sears, P. Lambrianides, H. B. Shore, Statistics of spectra of disordered systems near the metal-insulator transition, Phys. Rev. B 47 (1993) 11487–11490.
- [10] R. Berkovits, Y. Avishai, Spectral statistics near the quantum percolation threshold, Phys. Rev. B 53 (1996) R16125–R16128.

- [11] A. Kaneko, T. Ohtsuki, Three-dimensional quantum percolation studied by level statistics, *Journal of the Physical Society of Japan* 68 (1999) 1488–1491.
- [12] P. Mehta, M. Bukov, C.-H. Wang, A. G. Day, C. Richardson, C. K. Fisher, D. J. Schwab, A high-bias, low-variance introduction to machine learning for physicists, *Phys. Rep.* 810 (2019) 1.
- [13] G. Carleo, I. Cirac, K. Cranmer, L. Daudet, M. Schuld, N. Tishby, L. Vogt-Maranto, L. Zdeborová, Machine learning and the physical sciences, *Rev. Mod. Phys.* 91 (2019) 045002.
- [14] T. Ohtsuki, T. Mano, Drawing phase diagrams of random quantum systems by deep learning the wave functions, *J. Phys. Soc. Jpn.* 89 (2020) 022001.
- [15] E. Bedolla, L. C. Padierna, R. Castañeda-Priego, Machine learning for condensed matter physics, *Journal of Physics: Condensed Matter* 33 (2020) 053001.
- [16] T. Ohtsuki, T. Ohtsuki, Deep learning the quantum phase transitions in random two-dimensional electron systems, *Journal of the Physical Society of Japan* 85 (2016) 123706.
- [17] T. Ohtsuki, T. Ohtsuki, Deep learning the quantum phase transitions in random electron systems: Applications to three dimensions, *Journal of the Physical Society of Japan* 86 (2017) 044708.
- [18] P. Broecker, J. Carrasquilla, R. G. Melko, S. Trebst, Machine learning quantum phases of matter beyond the fermion sign problem, *Scientific Reports* 7 (2017) 8823.
- [19] J. Carrasquilla, R. G. Melko, Machine learning phases of matter, *Nature Physics* 13 (2017) 431–434.
- [20] Y. Zhang, E.-A. Kim, Quantum loop topography for machine learning, *Phys. Rev. Lett.* 118 (2017) 216401.
- [21] Y. Zhang, R. G. Melko, E.-A. Kim, Machine learning z_2 quantum spin liquids with quasiparticle statistics, *Phys. Rev. B* 96 (2017) 245119.
- [22] N. Yoshioka, Y. Akagi, H. Katsura, Learning disordered topological phases by statistical recovery of symmetry, *Phys. Rev. B* 97 (2018) 205110.
- [23] E. P. van Nieuwenburg, Y.-H. Liu, S. D. Huber, Learning phase transitions by confusion, *Nature Physics* 13 (2017) 435.
- [24] P. Zhang, H. Shen, H. Zhai, Machine learning topological invariants with neural networks, *Phys. Rev. Lett.* 120 (2018) 066401.

- [25] H. Araki, T. Mizoguchi, Y. Hatsugai, Phase diagram of a disordered higher-order topological insulator: A machine learning study, *Phys. Rev. B* 99 (2019) 085406.
- [26] D. Carvalho, N. A. García-Martínez, J. L. Lado, J. Fernández-Rossier, Real-space mapping of topological invariants using artificial neural networks, *Phys. Rev. B* 97 (2018) 115453.
- 180 [27] T. Mano, T. Ohtsuki, Phase diagrams of three-dimensional anderson and quantum percolation models using deep three-dimensional convolutional neural network, *Journal of the Physical Society of Japan* 86 (2017) 113704.
- [28] T. Mano, T. Ohtsuki, Application of convolutional neural network to quantum percolation in topological insulators, *Journal of the Physical Society of Japan* 88 (2019) 123704.
- [29] J. Chabé, G. Lemarié, B. Grémaud, D. Delande, P. Szriftgiser, J. C. Garreau, Experimental observation of the anderson metal-insulator transition with atomic matter waves, *Phys. Rev. Lett.* 101 (2008) 255702.
- 190 [30] G. Lemarié, J. Chabé, P. Szriftgiser, J. C. Garreau, B. Grémaud, D. Delande, Observation of the anderson metal-insulator transition with atomic matter waves: Theory and experiment, *Phys. Rev. A* 80 (2009) 043626.
- [31] M. Lopez, J.-F. Clément, P. Szriftgiser, J. C. Garreau, D. Delande, Experimental test of universality of the anderson transition, *Phys. Rev. Lett.* 108 (2012) 095701.
- [32] F. Haake, *Quantum signatures of chaos*, Springer, Berlin ; New York, 2010.
- [33] G. Casati, I. Guarneri, D. L. Shepelyansky, Anderson transition in a one-dimensional system with three incommensurate frequencies, *Phys. Rev. Lett.* 62 (1989) 345.
- [34] S. Hochreiter, J. Schmidhuber, Long short-term memory, *Neural Computation* 9 (1997) 1735–1780.
- 200 [35] C. Olah, Understanding lstm networks, <http://colah.github.io/posts/2015-08-Understanding-LSTMs/>, 2015.
- [36] T. Ohtsuki, T. Kawarabayashi, Anomalous diffusion at the anderson transitions, *Journal of the Physical Society of Japan* 66 (1997) 314–317.